The Scientific Journal of University of Benghazi

http://journals.uob.edu.ly/sjuob

Effect of Er2O3 and ErF3 on the optical properties of sodium oxyfluoroborate glasses

Ibrahim Z. Hager [1 *], Ibrahim A. Saleh [2]

1 Physics Department, Faculty of Science, Menoufia University, Shebin El-Koom, Egypt.
2 Physics Department, Faculty of Arts and Science, Al Abyar, Benghazi University, Libya.

Received 05 / 07 / 2022; Accepted 12 / 12 / 2022

الملخص

جهزت عينات زجاجية طبقا للتركيب B2O3Na2ONaF وطعمت بأكسيد الاربيوم Er2O3 وفلوريد الاربيوم ErF3، وذلك بطريقة التبريد المفاجئ للمصهور، ثم قيست الكثافة الحجمية وحُسب الحجم المولارى للعينات المحضرة. وُجد ان قيم الكثافة الحجمية والحجم المولارى يزداد بزيادة محتوى ErF3,Er2O3 ثم قيست أطياف الامتصاص الضوئي وذلك لدراسة الخواص الضوئية واعتمادها على المحتوى ErF3,Er2O3 للعينات الزجاجية المحضرة. كما حُسب معامل الانكسار الضوئي ودرس اعتماده على كل من الطول الموجي المطبق والمحتوى ErF3,Er2O3 والكثافة الحجمية وكذلك على نسبة ذرات الأكسجين الى ذرات الفلور O/F كما حُسب معامل الانكسار الغير خطي، والقابلية الضوئية والمغناطيسية، وعدد آبى والانكسار المولارى، وقابلية الاستقطاب الإلكتروني، وكذلك طاقة الفجوة الضوئية وربط ودراسة جميع هذه الخواص بمحتويات ErF3,Er2O3

الكلمات المفتاحية: زجاج بورات الاوكسي فلوريدي، طيف الامتصاص، ايونات العناصر الارضية، معامل الانكسار، الثوابت الضوئية.

Abstract

Glasses based on B_2O_3–Na_2O–NaF doped with Er_2O_3 and ErF_3 were prepared by the melt quench technique. Density was measured and molar volume was calculated. The density and molar volume increased with the increase of Er_2O_3 and ErF_3 content. Optical absorption spectra were measured to study the optical properties and their dependence on the Er_2O_3 and ErF_3. The refractive index is estimated and correlated with the wavelength, Er_2O_3, ErF_3, density, and O/F ratio. Nonlinear refractive index, optical and magnetic susceptibilities, Abbe number, molar refractivity, electronic polarizability, and energy gap were also calculated and correlated with Er_2O_3 and ErF_3 contents.

Keywords: Borate oxyfluoride glass, Absorption spectra, rare earth ion, refractive index, optical constants.

1. INTRODUCTION

Oxide glasses are attracting hosts for obtaining efficient luminescence in rare-earth ions. In them, borate glass is a suitable optical material with high transparency, low melting point, high thermal stability, and good rare-earth ions solubility [1,2,3].

The research for excellent hosts still attracts much attention from scientists. At present, heavy metal oxyfluoride glass [4,5,6,7] is considered to be one of the most promising materials because it can well combine good optical, mechanical and thermal-stable properties of the oxides with lower phonon energy of fluorides which can effectively reduce multiphonon decay of excited states in rare-earth ions and thus enhance the optical quantum efficiency [8,9,10].

Rare-earth ion-doped glasses are technologically important materials as they can be applied in lasers, white light-emitting diodes, light-converting, and optoelectronic devices [11, 12,13,14]. The optical properties of rare-earth ions in various glass systems like silicates, phosphates, borates, germinates, tellurites, fluorides, etc. have been studied and reviewed in the literature [14,15.16,17,18]. These ions can exist in different environments in the glass matrix; the study of the environment around the rare-earth ion is essential to understand the optical absorption and luminescent properties of rare-earth ion-doped glasses.

***Correspondence**: Ibrahim Z. Hager
E-mail: izhager@yahoo.com

Optical methods like UV-visible and infrared spectroscopy can give the average coordination number, bond lengths, local symmetry, or covalency of bonds between the rare-earth ion and the first shell neighbors [19]. Borate glasses are structurally more intricate as compared to silicate or phosphate glasses due to two types of coordination of boron atoms with oxygen (3 and 4). It is well established that the addition of metal oxides converts the boron coordination and the structural groups from one to another depending on the type and concentration of the metal oxides [20,21,22]. For special optical applications, the role of glasses as ultraviolet (UV) transmitting materials has increased in the last decade. The real UV transmission is limited by extrinsic charge transfer and s-p absorption bands due to trace impurities of metal ions such as Fe^{3+}/Fe^{2+}, Pb^{2+}, etc., which are influenced by the glass matrix [23, 24].

The refractive index as a function of wavelength is a critical design parameter for advanced photonic systems. Thus, the ability to estimate the refractivity of glasses based solely on their composition is of great value to both photonic designers and the materials scientists supporting those designs. Usually, the refractive index is known or measured, and then the polarizability is calculated, such as with the Lorentz–Lorenz equation [25, 26].

In the present oxyfluoroborate glasses doped with Er_2O_3 and ErF_3, the refractive index is calculated and correlated with the wavelength in the UV–VIS range. The molar refractivity, nonlinear refractive index, electronic polarizability, Abbe number, energy gap, and absorption cross-section of the glasses

 ISSN:Online 2790-1637, Print 2790-1629; National Library of Libya, Legal number : 154/2018

were calculated for different wavelengths. The effect of Er_2O_3 and ErF_3 on the determined optical properties is discussed.

2. EXPERIMENTAL TECHNIQUES:

The glasses were prepared from appropriate mixtures of H_3BO_3, Na_2O, NaF, Er_2O_3, and ErF_3. The batches were inserted into the furnace at 950 °C for 30 min in a platinum crucible and then poured into a brass mold to obtain bar samples with dimensions of 1 x 1 x (0.6-0.65) cm^3. Each glass sample was annealed near its glass transition temperatures, which depend on its composition for 1 h. Then the furnace was switched off and the sample was taken out after 24 h and prepared for measurements.

The densities of the prepared samples were measured by the Archimedean method using CCl_4 as an immersion liquid. The molar volume was calculated by the equation $V_m = (M/\rho)$, where ρ is the density and M is the molecular weight of the glass sample which is calculated as follows: $M = \sum_i (x_i)(w_i)$, where x_i and w_i are the mole fraction and molecular weight of component i, respectively. The error of the density measurements was not more than ±0.001 gm/cm^3.

The optical absorption spectra of the samples were recorded using T80 UV/VIS double beam spectrophotometer (PG Instruments Ltd) in the range from 190 to 700 nm. The refractive indices of the obtained glasses were calculated from the UV absorption spectra.

3. RESULTS:

The values of the glass composition, density, average molecular weight, molar volume, Er ion concentration per cm^3, and oxygen/fluorine O/F ratio of the present glasses are reported in Table 1. Fig. 1 shows the increase of the density and the molar volume with the increased of both Er_2O_3 and ErF_3 instead of Na_2O contents [27,28].

Table 1 Glass composition in mol%, density in gm/cm^3, average molecular weight, molar volume in cm^3, the concentration of Er ion per cm3, and oxygen/fluorine ratio of the present glasses.

Sample No.	B_2O_3 mol%	NaF mol%	Na_2O mol%	Er_2O_3 mol%	ErF_3 mol%	ρ gm/cm^3	M	V_m cm^3/mol	n(Er) x10^{20} cm^{-3}	O/F
BNN-1ErO	70	15	14	1		2.387	67.535	28.293	4.257	15.15
BNN-2ErO	70	15	13	2		2.481	70.740	28.513	8.448	15.27
BNN-3ErO	70	15	12	3		2.601	73.945	28.430	12.709	15.41
BNN-1ErF	70	15	14		1	2.310	65.952	28.551	2.109	12.50
BNN-2ErF	70	15	13		2	2.355	67.575	28.694	4.197	10.64
BNN-3ErF	70	15	12		3	2.399	69.198	28.844	6.243	9.26

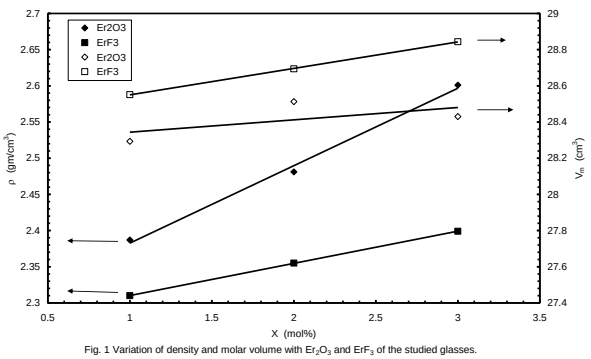

Fig. 1 Variation of density and molar volume with Er_2O_3 and ErF_3 of the studied glasses.

Fig. 2(A and B) shows the UV–VIS absorption spectra at room temperature in the range from 190–700 nm of the present glasses undoped and doped with both Er2O3 and ErF3 respectively. Absorption rises abruptly around a photon wavelength of 190 nm in all glasses depending on its composition. This wavelength is taken as optical absorption cut-off λ_o. The most intense absorption is produced by electronic transitions from the valence band to the conduction band of the crystal. These transitions give rise to absorption in the ultraviolet and are visible in the present oxyfluoroborate glasses doped with erbium ions (like silicates); they lead to intrinsic semiconduction when thermally excited. Several weak peaks were found at energies near those of the ultraviolet absorption edges; these correspond to energy in exciton absorption i.e. to

 ISSN:Online 2790-1637, Print 2790-1629; National Library of Libya, Legal number : 154/2018

transitions involving levels between the valence and conduction bands. They are too weak and at too high frequencies to be interpreted as due to lattice vibrations.

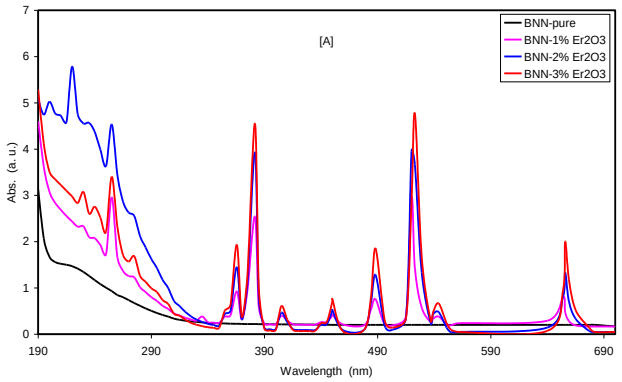

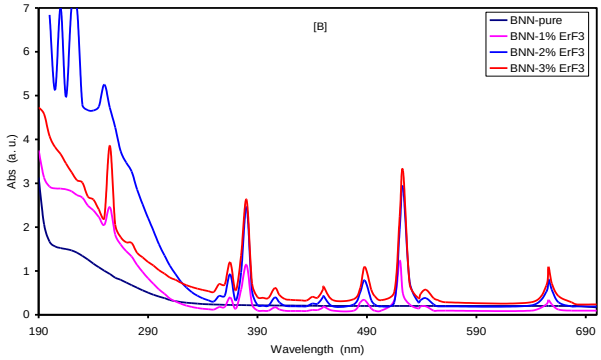

Fig. 2 Absorption spectra of: [A]Er_2O_3 and [B]ErF_3 doped glasses.

The absorption peaks are at the same wavelength positions for Er_2O_3 and ErF_3 doped glasses while their intensity is higher for Er_2O_3 than ErF_3 doped glass. The increase of the intensity of the observed absorption bands with the increase of both Er_2O_3 and ErF_3 is shown in Fig. 3.

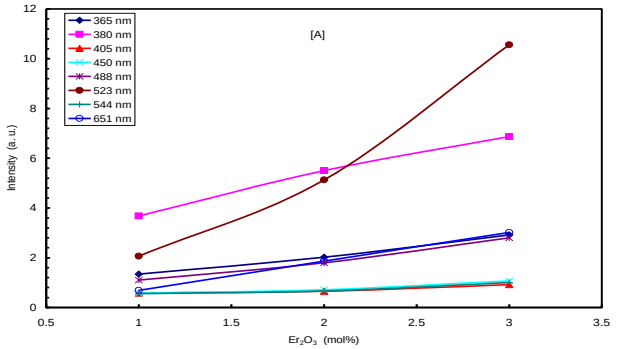

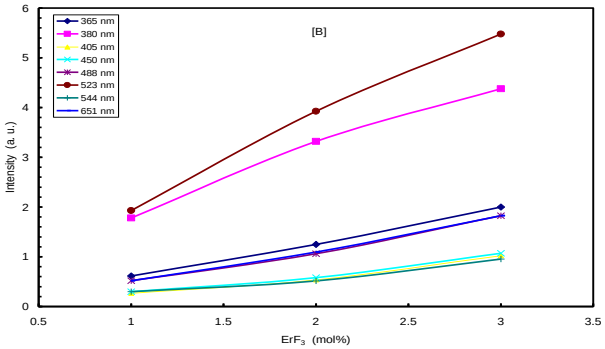

Fig. 3 Variation of the absorption intensity with: [A]Er_2O_3 and [B]ErF_3 content of the present glass.

The refractive index, n, of a material is an important parameter for the design of glass-related devices [30]. According to the theory of reflectivity of light (Fresnel's theory), the real part of *n* of the complex refractive index as a function of reflectance, R, and extinction coefficient, K, in the UV-VIS range is given by the quadratic equation,

$$R=\frac{(n-1)^2+K^2}{(n+1)^2+K^2}$$

where the appropriate root of the above equation is considered as the refractive index. The

extinction coefficient, K, is determined by,

$$K=\frac{\alpha\lambda}{4\pi}$$

where λ is the wavelength and α is the absorption coefficient of the material which is given by,

$$\alpha=\frac{2.303}{d}A$$

where *A* is optical absorption and *d* is the sample thickness in cm.

The correlation between *n* and the wavelength in the UV-VIS range is shown in Fig. 4(A and B). The values of *n* corresponding to the spectral line element are calculated and given in Table 2.

 ISSN:Online 2790-1637, Print 2790-1629; National Library of Libya, Legal number : 154/2018

Table 2 Refractive index according to the spectral line element and the dispersion of the present glasses.

Spectral line (nm)	Refractive index					
	BNN1ErO	**BNN2ErO**	**BNN3ErO**	**BNN1ErF$_3$**	**BNN2ErF$_2$**	**BNN3ErF$_3$**
C (656.3)	3.19538	2.63006	2.25549	3.43121	2.98382	2.76532
C$'$ (643.8)	3.31329	3.45202	3.49017	3.66358	3.45549	3.35838
D (589.3)	3.50751	3.72254	3.76763	3.70520	3.57341	3.46243
d (587.6)	3.51445	3.72601	3.77457	3.70173	3.56994	3.47630
e (546.1)	3.42428	3.36185	3.18844	3.61156	3.40694	3.21272
F (486.1)	3.07746	2.80000	2.58150	3.43815	3.06358	2.90405
F$'$ (479.9)	3.46243	3.49711	3.46936	3.62890	3.42081	3.29942
g (435.8)	3.53526	3.68786	3.71561	3.70867	3.58035	3.41387
h (404.6)	3.35491	3.28902	3.19191	3.62890	3.38266	3.16416
i (365.01)	2.88324	2.55723	2.29364	3.34451	2.84509	2.63353
ν_d		16.021	8.489	389.798	32.264	17.749
ν_e	6.447	5.9364	5.393	29.5171	16.9893	19.1505
ν_D	6.5424	6.5536	6.4605	30.1931	17.8643	20.9129

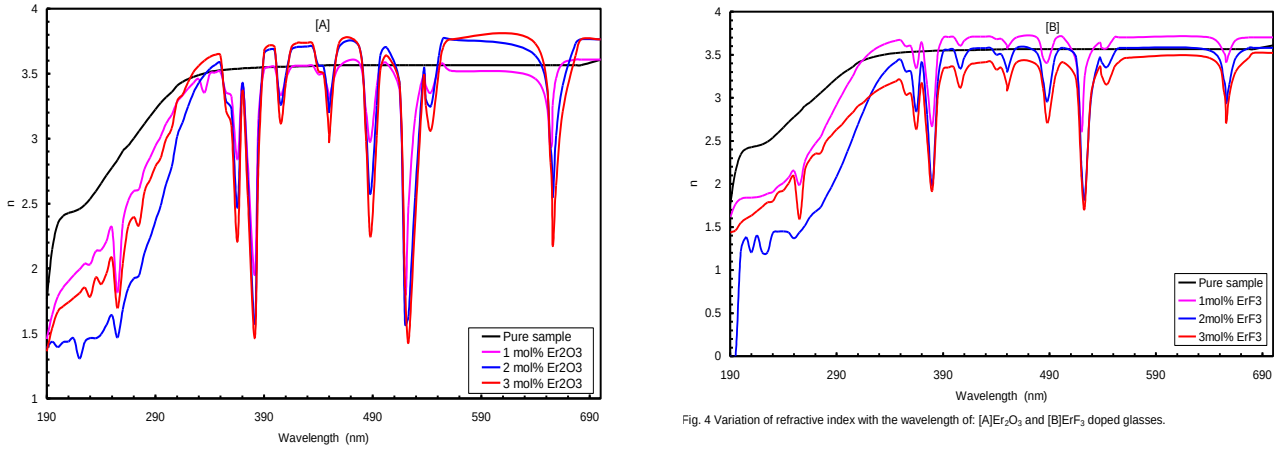

Fig. 4 Variation of refractive index with the wavelength of: [A]Er_2O_3 and [B]ErF_3 doped glasses.

The variation of the refractive index, *n*, at the different spectral line elements with the composition of Er_2O_3 and ErF_3 is shown in Fig. 5.

Fig. 6 shows the variation of the refractive index with the density.

 ISSN:Online 2790-1637, Print 2790-1629; National Library of Libya, Legal number : 154/2018

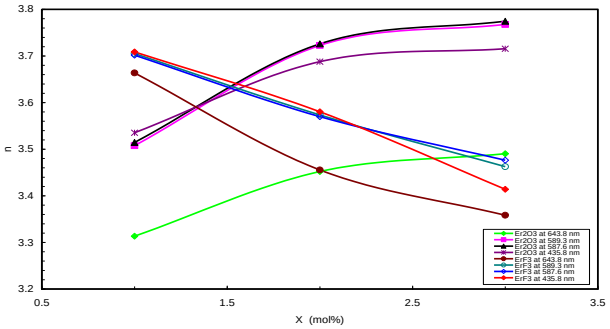

Fig. 5 Variation of refractive index at different wavelengths with the composition of the present glasses.

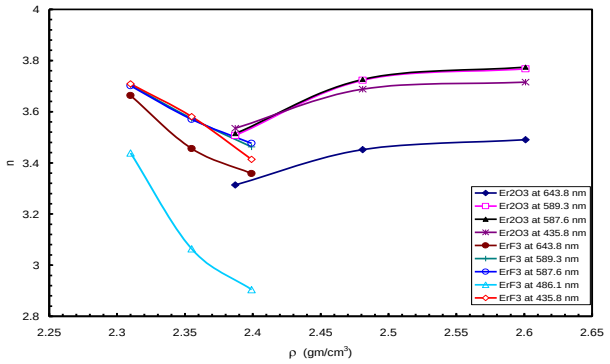

Fig. 6 Variation of refractive index at different wavelength with density of the glasses.

Fig. 7 [A and B] shows the variation of the refractive index at different wavelengths with the O/F ratio [31]. It is seen that *n* increase with the O/F ratio for Er_2O_3 while the decrease for ErF_3 glasses (remember that O/F decreases in ErF_3 doped glass, Table 1). It is known that in oxyfluoride glasses, the oxygen/fluorine (O/F) ratio is the most important effect parameter for determining the glass structure and physical properties. The incorporation of F^- ions creates, more network terminating sites and in turn produces interstitial spaces for accommodating large cations (e.g. La^3, Pb^2 in silicate [16] and Er^{3+} in the studied borate glasses). The incorporation of fluorides was therefore a means to enhance the solubility of lanthanides in the silicate and also the present oxyfluoroborate matrix, which is why the effect of F^- ions (referred to as the O/F ratio) is the best way to represent the network modifying parameter, on which many of the physical, structural, and spectroscopic properties depend. Since F^- creates interstitial spaces, so by doping Er_2O_3 instead of Na_2O of the present glasses the fluorine ion decrease (or oxygen ion increases) and the interstitial spaces will decrease, and the packing increase. This will decrease the velocity of the penetrating light across the glass, therefore the refractive index increase.

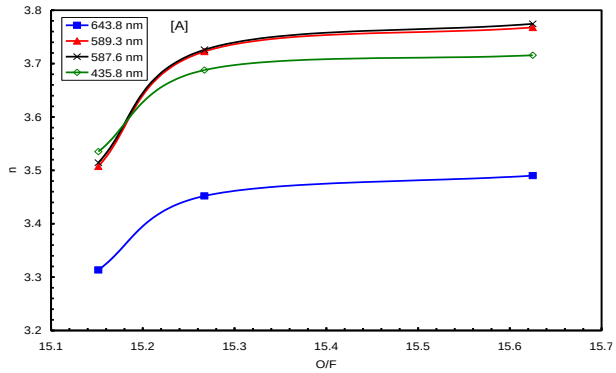

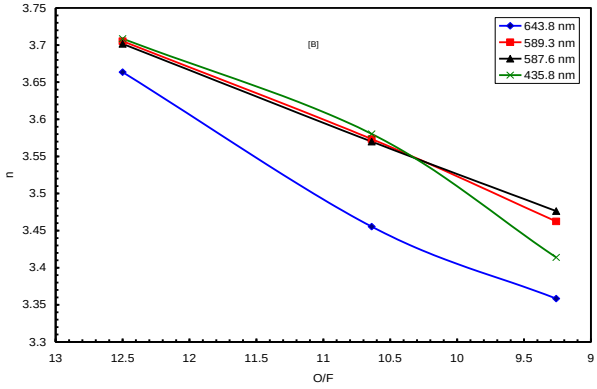

Fig. 7 Variation of refractive index with O/F ratio of [A] Er2O3 and [B] ErF3 doped glasses.

The refractive index of a glass is related through dielectric susceptibilities of cation-anion pairs present in the glass host. On the other hand, the presence of ionic bonds, such as those found in fluorides; reduces the refractive index due to the localization of electrons. This can be supported by calculating theoretically both optical, χ, and magnetic, χ_d, susceptibilities as follows [32,33].

$$\chi = 0.08\{[-\ln(0.102\Delta\chi^*)]^2 - 1\}$$

where $\Delta\chi^*$= (electronegativity of anion) – (electronegativity of cation).

$$\chi_d = -(8.82x10^{18}\, x\alpha_e + 5.02x10^{-6})$$

where α_e is the electronic polarizability is given by,

$$\alpha_e = 0.395x10^{-24}\left[\frac{4.207+k}{7.207+k}\right]\frac{M}{\rho}$$

and

$$k = \ln\Delta\chi^*(\ln\Delta\chi^* - 4.564)$$

The above parameters were calculated and their values are reported in Table 3.

 ISSN:Online 2790-1637, Print 2790-1629; National Library of Libya, Legal number : 154/2018

Table 3 Optical susceptibility, polarizability, magnetic susceptibility, nonlinear refractive index, and non-linearity refractive index coefficient of the present glasses.

Sample No.	χ	α x 10^{-24} cm^{-3}	χ_d x 10^{-6} $cm^3.mol^{-1}$	n_2 x10^{-11} esu	γ x10^{-15} cm^2/W
BNN-1ErO	0.1710	4.1158	-41.3127		
BNN-2ErO	0.1714	4.1428	-41.5455	3.9099	4.397
BNN-3ErO	0.1717	4.1697	-41.7783	10.5259	11.697
BNN-1ErF	0.1706	4.0845	-41.0413	0.03224	0.0366
BNN-2ErF	0.1704	4.0801	-41.0027	1.16479	1.365
BNN-3ErF	0.1702	4.0757	-40.9641	2.49245	3.014

The values of χ and χ_d of the present glasses are acceptable compared with those obtained for other glasses [34,35]. The refractive index of a glass depends on individual ions present in the glass and also the polarizability of cations. In general, the refractive index increases for highly polarizable cations. So that, the polarizability, me, of the present glasses is calculated to confirm this interpretation. Firstly, the molar refraction R_m is calculated and then α_{me} [36-38] as follows,

$$R_m = \left(\frac{n^2-1}{n^2+2}\right)V_m \qquad (7)$$

where $\left(\frac{n^2-1}{n^2+2}\right)$ called the molar refraction loss,and V_m is the molar volume of the glass. As the refractive index and molar volume increase, the corresponding increase in the molar refractive index can be predicted from Eq. (7). The calculated values of R_m at different spectral line elements are given in Table 4.

Table 4 Molar refractivity (cm3.mol-1) and polarizability (cm3) at C', d, e, F' and g lines of the present glasses.

Sample No.	R_m ($cm^3.mol^{-1}$)					Polarizability x 10^{-24} (cm^3)				
	C ' (643.8) nm	d (587.6) nm	e (546.1) nm	F ' (479.98) nm	g (435.8) nm	C ' (643.8) nm	d (587.6) nm	e (546.1) nm	F ' (479.98) nm	g (435.8) nm
BNN-1%Er_2O_3	21.669	22.356	22.065	22.127	22.502	8.586	8.877	8.756	8.804	9.125
BNN-2%Er_2O_3	22.208	23.179	22.062	22.402	23.009	8.791	9.175	8.742	8.899	9.125
BNN-3%Er_2O_3	22.062	23.106	21.431	22.159	22.836	8.811	9.165	8.516	8.811	8.901
BNN-1%ErF_3	22.956	23.094	22.858	22.917	23.094	9.098	9.151	9.061	9.061	9.166
BNN-2%ErF_3	22.527	22.873	22.314	22.394	22.819	8.924	9.077	8.825	8.879	9.077
BNN-3%ErF_3	22.166	22.694	21.837	22.079	22.496	8.829	8.986	8.630	8.769	8.907

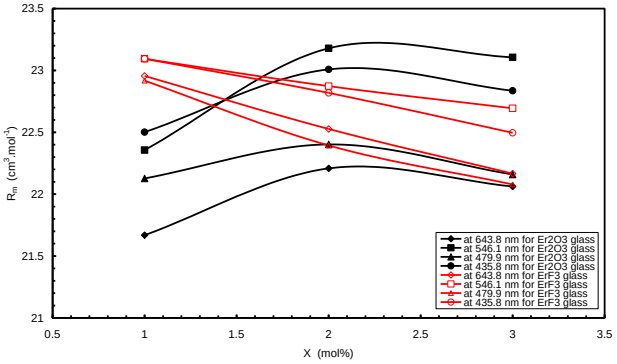

Fig. 8 Variation of molar refraction with Er_2O_3 and ErF_3 of the present glasses.

The molar refractive index is related to the structure of the glass and it is proportional to the molar electronic polarizability of the material, α_{me}, (in cm3 x 10-24) through the following Clasius-Mosotti relation,

$$\alpha_{me} = \left(\frac{3}{4\pi N}\right)R_m$$

where N is the number of polarizable ions per mole and is assumed equal to Avogadro's number NA.

The calculated values of α_{me} at different spectral line element wavelengths are given in Table 4.

 ISSN:Online 2790-1637, Print 2790-1629; National Library of Libya, Legal number : 154/2018

It is observed that α_{me} at different wavelengths increases with Er2O3 while it decreases in the case of ErF3 doped glass as shown in Fig. 9.

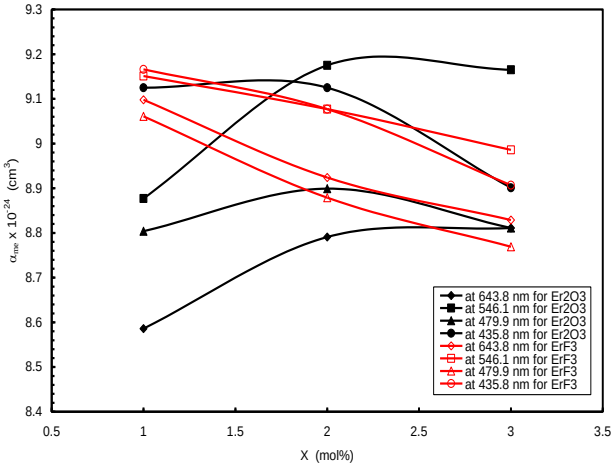

Fig. 9 Variation of molar electronic polarizability with Er_2O_3 and ErF_3 of the present glasses.

The energy gap E_g can calculate from [39,40].

$$E_g = 20\left(1-\frac{R_m}{V_m}\right)^2$$

$$E_g = \left[1.23\left(1-\frac{R_m}{V_m}\right)+0.98\right]^2$$

The energy gap, see Table 5 and Fig. 10 [31].

Table 5 Energy gap at different wavelengths of the present glasses.

Sample No.	E_g (eV), Eq.(9)				E_g (eV), Eq.(10)			
	C' (643.8 nm)	e (546.1 nm)	F' (479.98 nm)	g (435.8 nm)	C' (643.8 nm)	e (546.1 nm)	F' (479.98 nm)	g (435.8 nm)
BNN-1%Er_2O_3	1.2030	0.9266	0.8203	0.8356	1.6427	1.5494	1.5107	1.5164
BNN-2%Er_2O_3	2.0055	0.9341	0.7309	0.7309	1.6078	1.5521	1.4766	1.4766
BNN-3%Er_2O_3	1.1144	1.0903	0.7309	0.7114	1.6128	1.6058	1.4766	1.4689
BNN-1%ErF_3	0.7957	0.7741	0.7309	0.7234	1.5015	1.4933	1.4766	1.4736
BNN-2%ErF_3	1.0009	0.9413	0.8678	0.8236	1.5754	1.5546	1.5282	1.5119
BNN-3%ErF_3	1.1224	1.1319	0.9954	0.9605	1.6164	1.6196	1.5735	1.5614

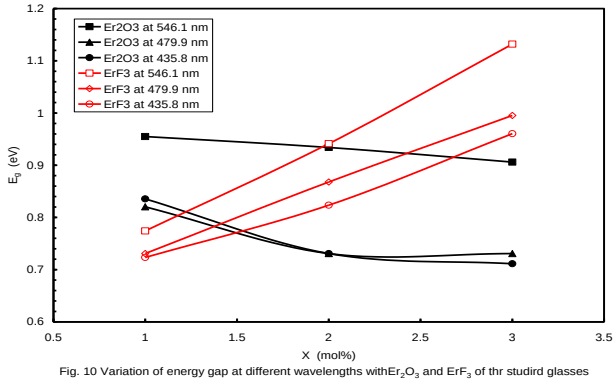

Fig. 10 Variation of energy gap at different wavelengths withEr_2O_3 and ErF_3 of thr studird glasses

The most important quantities for applications in the visible spectral range are:

- the central relative refractive index for the d line n_d (formerly also n_D or n_e had been chosen),
- the central dispersion (n_F-n_C),
- and the inverse of the dispersion relative to the refractive power, i.e., the Abbe number, ν_d, which is given by,

$$\nu_d = \frac{n_d - 1}{n_F - n_C}$$

Formerly, also $\nu_e = (n_e-1)/(n_{F'}-n_{C'})$ and $\nu_D=(n_D-1)/(n_{F'}-n_{C'})$ were used. All the above optical quantities are calculated and given in Table 2. The interpretation of the Abbe number is quite simple: It quantifies in the visible range how many times the average deviation angle of a prism is larger than the spread angle of the white light. Thus, a large (small) Abbe number characterizes a relatively small (large) spread. There is an inverse relationship between the Abbe number and the refractive index in the optical glasses, which means the glass with a relatively high refractive index, has a relatively low Abbe number.

 ISSN:Online 2790-1637, Print 2790-1629; National Library of Libya, Legal number : 154/2018

Another interesting matter is the non-linearity refractive index, n_2, which is evaluated from [41].

$$n_2(10^{-13}\,esu) = \left[\frac{68(n_d - 1)(n_d^2 + 2)^2}{\nu_d \left[1.517 + \frac{(n_d^2 + 2)(n_d + 1)\nu_d}{6n_d} \right]^{1/2}} \right] \quad (12)$$

On evaluating this factor, it is easy to compute the non-linearity refractive index coefficient, γ, as follows [42] :

$$\gamma\,(cm^2/W) = \frac{4\pi x 10^7}{c\,n_d}\, n_2(esu) \quad (13)$$

where n_d is the refractive index at 589.3 nm,and c is the velocity of light. The values of n_2 and γ are given in Table 3.

4. Discussion

The values of the glass composition, reported in Table 1. Fig. 1 shows the increase of the density is attributed to the molecular weight of both Er2O3 and ErF3 being higher than that of Na2O, while the increase in molar volume is attributed to the increase of the B–B and then B–O bond length as discussed in our previous work [29].

From Figs. 2 (A and B) that the obtained absorption peaks are due to the electronic transition of the Er3+ ion from the ground state 4I15/2 [27] since the pure sample lacks any absorption peaks. These absorption bands which observed at 230 nm (43478 cm-1), 255 nm (39216 cm-1), 365 nm (27397 cm-1), 381 nm (26246 cm-1), 405 nm (24691 cm-1), 450 nm (22222 cm-1), 488 nm (20492 cm-1), 520 nm (19231 cm-1), 544 nm (18382 cm-1) and 655 nm (15267 cm-1) respectively are due to the transitions from the 4I15/2 ground state of Er3+ ion[27], to the various excited states of Er3+ ion which are: 4G9/2, 4G11/2, 2H9/2, 4F3/2, 4F7/2, 2H11/2, 4S3/2 and 4F9/2 respectively. We see shown in Fig. 3. increase of the intensity of the observed absorption bands with the increase of both Er2O3 and ErF3 This behavior is attributed to the increase of the Er3+ ion concentration per cm3 from 4.257–12.709x1020 and 2.109–6.243 x1020 cm-3 for Er2O3 and ErF3 doped glasses respectively (see Table 1), which may absorb more energy to pumps from the ground energy state to the higher excited energy states.

The variation of the refractive index, n, is shown in Fig. 5. It is observed that the refractive index increases with the increase of Er2O3 content while it decreases with ErF3 content. This may be due to that by adding Er2O3 instead of Na2O the concentration of oxygen ions is increased while adding ErF3 will decrease O2- and increase F- ions (see Table 1). Since O2- has high polarizability (3.88) than that of fluorine ion (1.04), therefore refractive index increased in the case of Er2O3 while it decrease in the case of ErF3 doped glasses. Fig. 6 shows the variation of the refractive index with the density.

It is observed that the refractive index increase in the case of Er2O3 doped glass while it decreases with the density of ErF3 doped glass. This is due to the effect of the packing density of the glass [29].

Therefore the relationship between the refractive index and the O/F ratio, as shown in Fig. 7 [A and B], is a combination of the two effects: the structural packing of the glass networks with large and small cations and the localization/ delocalization of electrons due to the nature of local bonds[31].

The values that both optical and magnetic susceptibilities are increased from 0.1710-0.1717, (-41.3127)-(-41.7783)x10-6 (cm3.mol-1) for Er2O3 containing glass while decrease from 0.1706-0.1702, (-41.0413)-(-40.9641) x10-6 (cm3.mol-1) for ErF3 doped glass. This is another reason that the refractive index is increased in Er2O3 doped glass while it decreased in ErF3 doped glass.

The value of R_m , α_{me} and n is increased with the increase of the Er2O3 in the glass while it decreased in the case of ErF3 doped glass. The optical energy gap decrease with increasing cationic size (or anionic size). Referring to the O/F ratio its value is higher in the case of Er2O3 doped glass than in ErF3 glass. And since the ionic radius of O2 – (1.40 Å) is greater than F- ion (1.26 Å). Therefore E_g is decreased by increasing Er2O3 than ErF3 contents. The values of n_2 and γ are increased with increasing of both Er2O3 and ErF3.Their values are acceptable compared with the other glasses [43,44].

5. REFERENCES:

1. Isabella-Ioana Oprea, Hartmut Hesse, Klaus Betzler, Optical Materials 26 (2004) 235.
2. P. Becker, Advanced Materials 10 (1998) 979.
3. N. Soga, K. Hirao, M. Yoshimoto, H. Yamamoto, J. Appl. Phys. 63 (1988) 4451.
4. S.M. Kaczmarek, Opt. Mat. 19 (2002) 189.
5. Lina, H., Yanga, D., Liua, G., Maa, T., Zhaia, B., Ana, O., Yua, J., Wangb, X., Liub, X., Edwin Yue-Bun Pun, E. Y-B., Lumin, J. 113 (2005) 121.
6. Feng, L., Wang, J., Tang, Q., Hu, H., Liang, H., Su, Q. J. Non-Cryst. Solids 352 (2006) 2090.
7. Hager, I. Z., J. Phys. Chem. Solids 70 (2009) 210.
8. Yang, J., Zhang, L., Wen, L., Dai, S., Hu, L., Jiang, Z. J. Appl. Phys. 95 (2004) 3020.
9. Nazabal, V., Todoroki, S., Inoue, S., Matsumoto, T., Suehara, S., Hondo, T., Araki, T., Cardinal, T. J. Non-Cryst. Solids 326–327 (2003) 359.
10. Silva, M. A. P., Messaddeq, Y., Briois, V., Poulain, M., Riberiro, S. J. L. J. Phys. Chem. Solids 63 (2002) 605.
11. Xu, S., Yang, Z., Wang, G., Dai, S., Zhang, J., Hu, L., Jiang, Z. J. Alloys Compd. 377 (2004) 253.
12. Xu, S., Wang, G., Zhang, J., Dai, S., Hu, L., Jiang, Z. J. Non-Cryst. Solids 336 (2004) 230.
13. Campbell, J. H., Suratwala, T. I. J. Non-Cryst. Solids, 263-264 (2000) 318.

 ISSN:Online 2790-1637, Print 2790-1629; National Library of Libya, Legal number : 154/2018

14. Jackson, S. D., Appl. Phys. Lett., 83 (2003) 1316.

15. Zheng, Y. Clare, Y. A. G. Phys. Chem. Glasses, 46[4] (2005) 467.

16. Bajaj, A., Khannaw, A., Kulkarni, N. K., Aggarwal, S. K.. J. Am. Ceram. Soc., 92 [5] (2009) 1036.

17. Balda, R., Fernandez, F., Sanz, M., de Pablos, A., Fdez-Navarro, J. M., Mugnier, J. Phys. Rev. B, 61 [5] (2000) 3384.

18. Hager, I. Z., El-Mallawany, R., Bulou, A. Phys. B 406 (2011) 792.

19. Reisfeld, R., Eckstein, Y. J. Solid State Chem., 5 [2] (1972) 174.

20. Gatterer, K., Pucker, G., Fritzer, H. P., Arafa, S. J Non-Cryst. Solids, 176 [2–3] (1994) 237.

21. Prasad, S., Clark, T. M., Sefzik, T. H., Kwak, H., Gan, Z., Grandinetti, P. J. J. Non- Cryst. Solids, 352 [26-27] (2006) 2834.

22. Shaw, J. L., Zwanziger, U. W., Zwanziger, J. W. Eur. J. Glass Sci. Technol., 47 [4] (2006) 513.

23. Ehrt, D., Ebeling, P., Natura, U., Kolberg, U., Naumann, K., Ritter, S. International Congress on Glass, vol. 1, Invited Papers, Edinburgh, Scotland, 2001, pp. 84–93.

24. Sigel, G. H., Ginther, R. J. Glass Technol. 9 (1968) 66.

25. Lorentz, H. A. Wied. Ann. 9 (1880) 641.

26. R. Lorentz, R. Wied Ann. 11 (1880) 70.

27. Yuliantini, L., Djamal, M., Hidayat, R., Boonin, K., J. Kaewkhao, Materials Today: Proceedings 5 (2018) 15076–15080.

28. Alothman, M. A., Kurtulus, R., Olarinoye, I. O., Kavas, T., Mutuwong, C., Al-Buriahi, M. S. Optik - International Journal for Light and Electron Optics 248 (2021) 168047.

29. Hager, I. Z. J. Alloys & Comp. 539 (2012) 256.

30. Neumann, H., Horig, W., Reccins, E., Sobotta, H., Schumann, B., Kuh, G. Thin Solid Films 61 (1979) 13.

31. Stalina, S., Gaikwadb, D.K. Sameea, M.A. Edukondalua, A. Ahmmadc, S. K., Joshib, A. A., Syeda, A. Ceramics International 46 (2020) 17325–17334.

32. Reddy, R. R., Ahammed, Y. N., Ramagopal, K., Raghuram, D.V. Opic. Mater.10 (1998) 95.

33. Singh, S., Singh, P. J. Phys. Chem. Solids 41 (1980) 135.

34. Djouama, T., Poulain, M., Soltan, M. T., Boutrafaia, A. J. Optoelectronic Adv. Mater. 1[3] (2009) 358.

35. Srinivasarao, G., Veeraiah, N. J. Phys. Chem. Solids 63 (2002) 705.

36. Natura, U., Feuer, T., Ehrt, D. Nucl. Instr. and Meth. B 166–167 (2000) 470.

37. Dumbaugh, W. H. ‘‘Oxide Glasses with Superior Infrared Transmission,’’ Proc. SPIE, 505, (1984) 97–101.

38. Volf, M. B. Glass Science, and Technology, vol. 7, Elsevier Amestrdam, 1984, p. 43.

39. Duffy, A. J. solid St. Chem. 62 (1986) 145.

40. Banu, T., Rao, K. K., Vithal, M. Phys. Chem. Glasses 44 (2003) 30.

41. Boling, N. L. Glass, A. J., Owyoung, A. .IEEE J. Quantum Electron. 14 (1978) 601.

42. Annapurna, K., Buddhudu, S. J. Solid State Chem. 93 (1991) 454.

43. 43 Ticha, H., Tichy, L. J. Optoelectronic Adv. Mater. 4[2] (2002) 381

44. Yousef, E. Al-Salami, A. F., Hotzel, M. Bull. Mater. Sci 35 [6] (2012) 961.

 ISSN:Online **2790-1637**, Print **2790-1629**; National Library of Libya, Legal number : **154/2018**